

QUASI-COHERENT INTERACTION OF PROTONS WITH  
 $^{28}\text{Si}$  AT  $T_p=1$  GEV

Institute of Theoretical and Experimental Physics, ITEP,  
117259 Moscow, Russia

M.P.Besuglov, B.M.Bobchenko, E.V.Bustritskaya, A.A.Vasenko, M.E.Vishnevsky,  
N.D.Galanina, K.E.Gusev, V.S.Demidov, E.V.Demidova, V.V.Zhurkin,  
I.V.Kirpichnikov, V.A.Kuznetsov, V.N.Markizov, M.A.Martemianov, A.A.Nedosekin,  
B.N.Pavlov, V.A.Sadyukov, A.Yu.Sokolov, A.S.Starostin, N.A.Khaldeeva

ABSTRACT

The total, elastic and inelastic cross-sections for quasi-coherent interactions of protons with  $^{28}\text{Si}$  have been measured using hadron-gamma coincidence method at the energy 1 GeV. The limits for the existence of long-lived excited states of the  $^{28}\text{Si}$  nucleus have been obtained in the range of energies from 0 to 0.8 GeV.

# 1 Introduction

Quasi-coherent hadron-nucleus interactions  $A(h, h')A^*$  which result in nucleus  $A$  excitation and hadron  $h$  either elastic scattered or transformed into a system of hadrons can provide information on the properties of nucleus as well as on the mechanism of hadron-nuclei interaction. The experimental study of quasi-coherent reactions was performed mostly at high accuracy magnetic spectrometers measuring the scattering angle and nucleus momentum transfer. Reactions with the excitation of certain levels were selected via the missing mass. The investigation was carried out in a narrow region of transferred energies, since at the excitation energies over  $\approx 10$  MeV the domination of nucleus disintegration processes does not allow to separate quasi-coherent reactions without nuclear states being fixed.

In this paper quasi-coherent reactions are investigated using the method of hadron-gamma coincidence based on a simultaneous registration of the leading hadron and instant  $\gamma$ -rays following the transition of an excited nucleus into the state with minimal excitation energy or into the ground state. The identification of reactions is carried out via the energy of registered  $\gamma$ . The kinematical parameters measured by the magnetic spectrometer are used for the analysis of hadron-nucleus reactions.

Such method does not limit the value of energy transferred by the scattering nucleus. The region of possible energy transfer include the region of elastic hadron interactions as well as the region where the production of  $\pi$ -mesons with total charge equal to zero is allowed by kinematic laws.

It is evident that in the first region the total amount of transferred energy is spend for the nucleus excitation. For the hadron energy about 1 GeV the excitation of three lowest levels with natural parity has been observed in LINP experiment ( [1] – [3]). These data were used later to obtain the distribution of the density of nuclear matter ( [4], [5]). Slightly above the threshold of nucleon production gigantic resonances can be found. Their excitation in quasi-coherent reactions is not yet investigated well enough although such experimental data would be important for the estimation of radiative decay probability of one- and multiphonon gigantic nuclear resonances. The first experimental evidence of the radiative decay of two-phonon resonances was obtained recently in nucleus-nucleus interactions [6]. In the same energy region the narrow resonance states discovered in 1982 and interpreted as the cluster oscillations in nuclear matter can be displayed ( [7]– [11]).

In the region of higher transferred energies where non-elastic processes of meson production are possible quasi-coherent reactions have not been extensively studied. The abnormal contribution of non-elastic processes with extra particle production was observed by the method of hadron-gamma coincidence for the reactions  $^{16}O(\pi, \pi X)^{16}O^*$  and  $^{40}Ca(\pi, \pi X)^{40}Ca^*$  ( [12], [13], [14]). Quasi-coherent  $\pi$ -meson production has been investigated only for the  $(\pi, Si)$  reaction [15], although a number of theoretical works indicate that for the understanding of the hadron-nuclei interaction mechanism other reactions must be studied. [16]. The existence of nuclei states with high excitation (180 MeV) has been assumed in [17] in order to explain the maximum in the energy transfer distribution in the charge-exchange reaction  $A(\pi, \pi\pi)X$ .

In the present work the quasi-coherent interaction  $^{28}Si(p, px)^{28}Si^*$  is investigated using the method of hadron-gamma coincidence in the region of transferred energies from 0 to 0.8 GeV in order to discover long-lived and highly excited nuclei levels with electromagnetic decay channels and to study the mechanism of meson production.

## 2 The experiment

The experiment was carried out at the ITEP proton synchrotron using MAGE (MAGnetic-GERmanium spectrometer).

### 2.1 . The beam

The proton beam was formed by the magnetic tract consisting of 3 rejecting magnets and 4 focusing magnetic lenses placed at the angle  $3.5^\circ$  to the direction of inner accelerator beam. Protons accelerated to the momentum of 1.83 GeV/c in the synchrotron scattered on inner Be target and falled into the magnetic tract. The beam intensity was  $10^6$  protons/sec per  $\approx 0.4$  sec. The momentum distribution of protons reaching the experimental target had a gaussian shape with the mean value of  $1.822 \pm 0.001$  GeV/c and the standard deviation of 0.026 GeV/c. The mean value depends on the beam tract tuning and can vary withing the limits of 0.015 GeV/c for different runs (the correspondent corrections were included in data analysis). The angle beam dispersion in the target area did not exceed  $1.2^\circ$ , the size of the beam spot was  $4 \times 4$  cm<sup>2</sup>.

### 2.2 . The set-up components

A schematic view of the MAGE spectrometer is presented in fig.1.

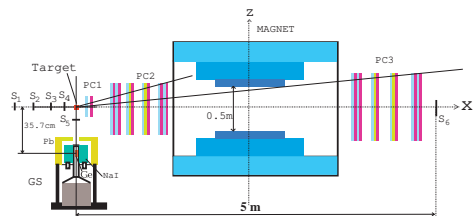


Figure 1: The side view of the MAGE spectrometer.

The MAGE spectrometer is a two-arm device. One arm is a magnetic spectrometer with proportional chambers, the second is a gamma-spectrometer based on a Ge(Li)-detector surrounded by a protection shield of NaI scintillation counters which is connected in anticoincidence with the detector.

### 2.2.1. The magnetic spectrometer

The magnetic spectrometer includes the magnet, track detectors and a system of scintillation counters. The working area of the magnetic field is  $0.5 \times 1 \times 1.8m^3$  with the field value in the center equal to 0.72 Tl.

The tracking part of the spectrometer consists of 30 plane multiwire proportional chambers [18] arranged in 3 groups: PC1, PC2 (placed between the target and the magnet) and PC3 (placed behind the magnet). The group PC1 includes 2 rectangular  $240 \times 240 mm^2$  coordinate planes with wires oriented transverse to the beam direction. The group PC2 includes 14  $480 \times 1280 mm^2$  planes: 6 with wires placed along the beam direction (z), 6 with transverse wires (y), in 2 planes wires are placed at the angle  $\approx 37^\circ$  with respect to the beam direction (w). The group PC3 used for the momentum measurements has the same structure as PC2 but the chamber size is  $880 \times 1840 mm^2$ . The distance between the signal wires is 2.5 mm, in slope planes - 2 mm, the total number of wires - about 15 000.

The proportional chambers are filled with the gas mixture  $Ar$  (70%) +  $CO_2$  (29,8%) +  $CF_3Br$  (0,2%).

The minimal measured momentum is 0.4 GeV/c, the precision of momentum measurement is  $\Delta p/p(\%) = 0.32p(\text{GeV}/c) + 0.57$ .

The target was placed 2.56 m from the center of the magnet. The maximum deviation angle of secondary charged particles registered by the spectrometer did not exceed 0.25 rad for the momentum measurements and increased to 0.55 rad when only PC1 and PC2 have been used.

The direction of charged secondary particles was measured with the precision of 0.002 rad, while the scattering angles with respect to the beam direction were determined with less precision (0.008 rad) because of the beam angle dispersion.

The system of scintillation counters  $S_1 - S_6$  was used to select the beam spot with the size of the target and to generate a signal of interaction of beam particles with the target. Together with the signal of  $\gamma$ -detector it is a part of the master signal triggering on-line data acquisition system based on VAX4200 connected with other computers by ETHERNET. The read-out electronics is described in [19] and [20]. The maximum rate of data acquisition is about 400 kb/sec.

### 2.2.2. Germanium $\gamma$ -spectrometer

The Ge(li)-NaI(Tl)  $\gamma$ -spectrometer (GS in fig.1) has been employed to register the instant photons following the deexcitation of atomic nuclei and to measure the  $\gamma$ -energy [21].

The spectrometer includes Ge(Li) detector with the volume  $100 cm^3$  placed in a cryostat and surrounded by a six-section NaI(Tl) shaft assembly of 300 mm height, 350 mm outer diameter and 100 mm shaft diameter connected in anticoincidence with the detector. Ge detector is placed 37.5 cm from the centre of the target. The scintillation counter  $S_5$  working in anticoincidence prevented the triggering of the spectrometer by charged particles. To reduce the outside background the spectrometer was surrounded by lead protection. The analog signal from the Ge detector was digitized by ADC and transferred to the computer. The monitoring of  $\gamma$ -spectrometer operation was performed by the 4096-channel NOKIA analyser.

The energy calibration of the Ge detector was performed using 18  $\gamma$ -lines of  $^{226}Ra$  in the range of energies from 180 to 3100 KeV. It was approximated by the function

$$E_{\gamma}(\text{keV}) = b(A_{gd} - a)^c, \quad (1)$$

where  $A_{gd}$  is the channel number of the amplitude analyser or ADC corresponding to the energy  $E_{\gamma}$ .

The values  $a=-48.45\pm 0.07$ ,  $b= 0.9532\pm 0.0007$ , and  $c=0.9849\pm 0.0003$  were estimated by the method of least squares.

The total  $\gamma$ -spectrometer efficiency depends on two factors:  $\Omega_{eff}(E_{\gamma}) = \Omega_g(E_{\gamma}) \cdot \eta(E_{\gamma})$ , where  $\Omega_g(E_{\gamma})$  is the geometric efficiency, and  $\eta(E_{\gamma})$  is the efficiency of the master signal.

To determine the geometric efficiency  $\Omega_g(E_{\gamma})$   $\gamma$ -spectra from 4 sources  $^{60}\text{Co}$ ,  $^{88}\text{Y}$ ,  $^{137}\text{Cs}$  and  $^{228}\text{Th}$  with well known intensities which cover the investigated energy range (0.5-3.0 MeV) have been measured by the spectrometer. The geometric efficiency was estimated for 8 experimental points by the method of least squares as  $\ln\Omega_g(\text{mster}) = (11.02 \pm 0.05) - (2.08 \pm 0.01)\ln E_{\gamma}(\text{keV}) + (0.0793 \pm 0.0007)\ln E_{\gamma}^2(\text{keV})$  with the precision less than 2%.

The introduction of the coefficient  $\eta(E_{\gamma})$  is connected with the use of time-gating for the reduction of the background. For runs with the target the "gate" duration was limited to  $\delta t=50$  nsec. Due to large fluctuations in the fore-front of Ge detector signal it was followed by the deterioration of the spectrometer efficiency. The efficiency  $\eta(E_{\gamma})$  was obtained by comparison of two  $\gamma$  spectra for  $\delta t=50$  nsec and  $\delta t=250$  nsec and approximated by the function  $\eta(E_{\gamma}) = 0.7 - 0.55 \cdot \exp(-0.017E_{\gamma}(\text{keV}))$ .

The dependence of  $\Omega_{eff}$  on photon energy is shown in Fig.2 in units of the "efficient" solid angle  $\Omega_{eff}$  covered by an ideal (detecting each photon)  $\gamma$ -detector.

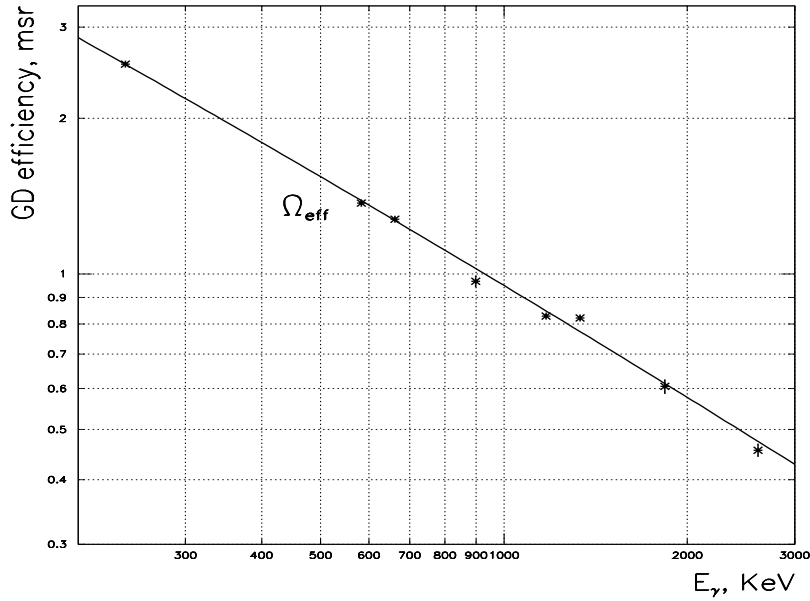


Figure 2: The dependence of Ge spectrometer efficiency on  $\gamma$  energy.

The anticoincidence signal from NaI allows to suppress the background in  $\gamma$ -spectrum of the Ge detector by a factor of 20-30 for runs with target (see fig.3).

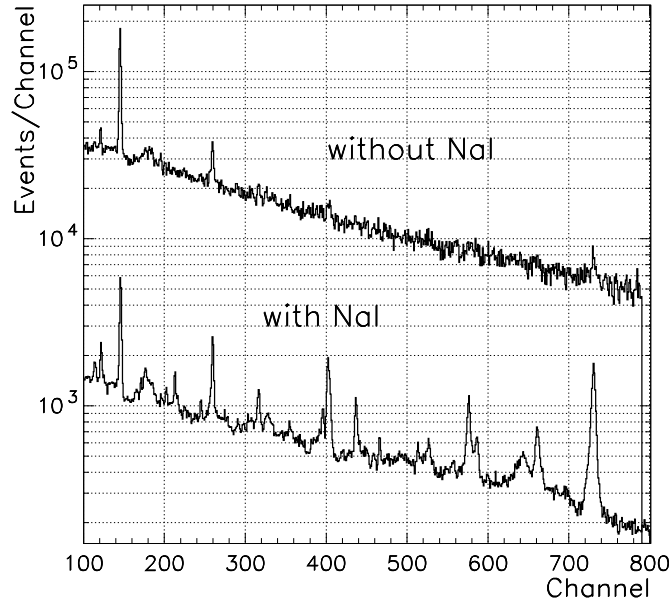


Figure 3: The suppression of background continuum by active NaI shield. Top histogram presents the region of  $\gamma$ -spectrum without active NaI protection, bottom - the same region with switched protection.

To estimate the systematic errors in cross-section measurements caused by the uncertainty in  $\gamma$ -spectrometer efficiency, the procedure of efficiency definition was repeated several times. It was found that the systematic errors do not exceed  $\pm 10\%$  while the basic contribution comes from the uncertainty in  $\eta(E_\gamma)$ .

The employment of Ge detector in our experiment has created a major difficulty which is the presence of background signals from charged particles and  $\gamma$ -quanta of higher energies. The amplitude overload of the spectrometer tract results in uncontrolled loss of spectrometer efficiency in case of the standard electronics, since the preamplifier signal has a duration of several milliseconds.

To prevent the overload the charge collection time defined by the preamplifier feedback circuit has been decreased by two orders. The energy resolution of Ge-detector (FWHM) was found to be 9-16 keV in the range of  $\gamma$  energies of 0.5-2.0 MeV and the shape of the detector response has been well approximated by Gaussian function.

To obtain the calibration dependence the average values for  $\gamma$ -lines of  $^{226}\text{Ra}$  spectrum have been used.

The limitation of the time delay of a registered signal from Ge detector with respect to a signal from scattered proton to the value of 50 nsec imposes an upper limit on the half-decay period  $T_{1/2}$  for the observed levels. Apparently the intensities of the levels with  $T_{1/2} \leq 10 \div 20 \text{ nsec}$  can be measured without distortion, for levels with higher  $T_{1/2}$  it is

necessary to take into account non-registered decays.

## 2.3 . Experimental procedure

Three runs have been carried out for 1.83 GeV/c proton beam directed at the center of a Si cylinder target with the diameter of 80 mm and the height of 27 mm. The isotopic structure of the target was the following:  $^{28}\text{Si}$ –92.23%,  $^{29}\text{Si}$ –4.67%,  $^{30}\text{Si}$ –3.1%, the density - 2.20 g/cm<sup>3</sup>. The interaction of protons with the most widespread isotope  $^{28}\text{Si}$  has been studied. For this isotope the quantum number of the ground state is  $0^+$ , the majority of higher excited nuclear states discharge through the first excited level ( $2^+$ ) with the energy 1.77003 MeV and half- decay period  $(686 \pm 13)10^{-15}$  sec [22]. The threshold energy of knocking out a nucleon from  $^{28}\text{Si}$  nucleus is  $E_t=11.58$  MeV.

To select all the events of proton interaction with the target followed by the detection of a photon in GS a master signal was generated according to the scheme  $S_1 S_2 S_3 S_4 \overline{S_5} S_6 \overline{\text{NaI}} \text{Ge}$ .

The counters  $S_1$ – $S_4$  limited the beam transverse size to  $4 \times 4$  cm<sup>2</sup>. The counter  $\overline{S_6}$ , connected in anticoincidence, rejected particles passing through the target without interaction in the angle  $\leq 0.4^\circ$ . The counter  $S_5$  and NaI-assembly provided the suppression of background in  $\gamma$ -detector.

The master signal triggers the work of the read-out system which transfers into the computer the addresses of the wires hit by charged particles, the amplitude  $A_{gd}$  of Ge detector signal and the indications of recount monitoring devices. The on-line information is send to data base accessible for subsequent off-line analysis.

To define the cross section of a nuclear reaction, the number of incident particles has been counted taking into account the dead time. For 3 runs with a total duration of 20 days this number was estimated to be  $N_o = 5.6 \times 10^{10}$  while the number of masters transferred into the computer was  $N_m = 1.18 \times 10^6$ .

## 3 . Data processing

### 3.1 . Preliminary data operation

Preliminary data operation has been made on Pentium-Pro (OS Linux) using MAGOFF code and included the reconstruction of the momentum of charged particles registered by the spectrometer, the definition of photon energy via the signal amplitude in the GS, the selection of events and the creation of the data base needed for further analysis.

In the present work the hadron-inclusive events (with one charged particle detected in the magnetic spectrometer) are analysed. The search of candidates was carried out among the events with simultaneous signals from at least 4 "y" planes and 3 "z" planes placed in front of the magnet, 3 "Y" and 2 "Z" planes behind the magnet. The particle momentum was defined after the "front" and "back" tracks were joined by the line which describes the trajectory in the relevant magnetic field.

Further selection of events was carried out according to the following criteria. If the number of extra signals from any of the 4 groups (y,z,Y,Z) exceeded 3, the event was rejected. It was shown by Monte-Carlo calculations that this algorithm permits to minimize the probable contribution of reactions with greater multiplicity as well as the contribution of the background events.

A total of  $0.242 \times 10^6$  one-track events were selected from  $1.18 \times 10^6$  masters. The information send to the data base included seven parameters for each 1-track event:  $X_{ti}, Y_{ti}, Z_{ti}$ - the measured coordinates of beam interaction point with the target nucleus,  $E_{\gamma i}$  - photon energy,  $p_i, \theta_i, \pi_i$  - the momentum of secondary particle and the angle after the interaction.

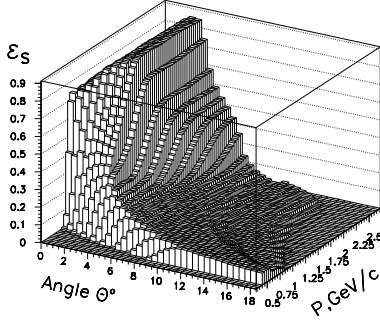


Figure 4: MAGE registration efficiency  $\varepsilon_s$  as a function of the angle and momentum.

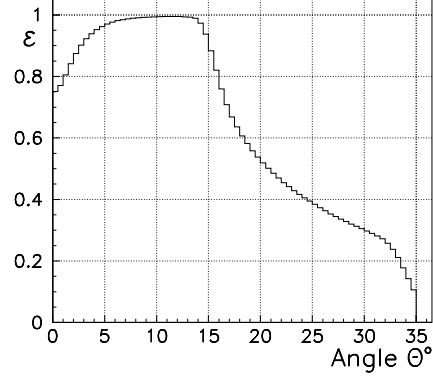


Figure 5: The efficiency  $\varepsilon$  of particle detection in forward blocks PC1 and PC2 as a function of the particle angle.

### 3.2 . The efficiency of the magnetic spectrometer

The efficiency of the magnetic spectrometer includes the geometric efficiency as well as the chamber efficiency  $W$  calculated for each working proportional chamber using MAGOFF code. For a number of chambers it was found to be dependent on the hit position:  $W = U(y, z)$ . This information was used in Monte-Carlo (GEANT) simulation of the spectrometer efficiency  $\varepsilon_s = f(\theta, p)$  as function of the angle and momentum of the particle emitted from the target. The efficiency  $\varepsilon = f(\theta)$  of particle registration by the forward blocks PC1 and PC2 has been also calculated. All the calculations were made for the uniform azimuthal distribution of secondary particles. The results are shown in fig.4 and fig.5.

The calculated efficiencies were taken into account in experimental data analysis where every  $i$ -th event was weighted by  $b_i(\theta_i, p_i) = 1/\varepsilon_{si}(\theta_i, p_i)$ .

### 3.3 . The excitation energy resolution of the spectrometer

The nucleus excitation energy  $\omega$  is one of the main parameters obtained for quasi-coherent scattering on nuclei. In the case of one leading particle it can be defined as the difference between the missing mass  $M^*$  in the reaction



and the rest mass  $M$  of the target nucleus:

$$\omega = M^* - M \quad (3)$$



The missing mass  $M^*$  can be expressed as

$$M^* = \sqrt{(E_0 + M - E)^2 - p_0^2 - p^2 + 2p_0p \cos\theta}, \quad (4)$$

where  $(E_0, p_0)$  and  $(E, p)$  - is the energy and the momentum of incoming and registered protons respectively. To analyze  $\omega$  spectra it is necessary to know the MAGE excitation energy resolution function  $g(\omega)$  which depends on the momentum resolution of the spectrometer as well as on the momentum dispersion of beam particles. The shape of the function (see Fig.6) was obtained from  $\omega$  distribution with excitation energy  $E^* = 0$  approximated by a sum of two Gaussian functions (smooth line):

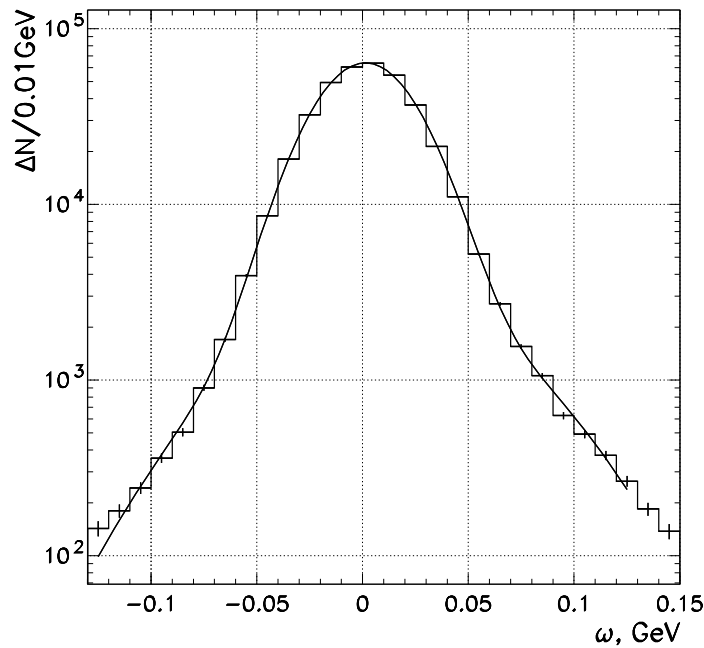


Figure 6: The excitation energy resolution function  $g(0, \omega)$ .

$$g(E^*, \omega) = \exp(-0.5((\omega - E^*)/(0.0225 \pm 0.0005))^2) + (0.075 \pm 0.001) \exp(-0.5((\omega - E^* + 0.0085 \pm 0.0003)/(0.0500 \pm 0.0007))^2). \quad (5)$$

where  $E^*$  is the energy of the observed excited level expressed in GeV.

The first term of this formula is responsible for 93% contribution and has a standard deviation of 0.0225 GeV. In the first approximation this value can be treated as the energy resolution of the magnetic spectrometer.

## 4. Measurement of the cross section of the reaction

$${}^{28}\text{Si}(p, px){}^{28}\text{Si}^* (E_\gamma = 1.78 \text{ MeV})$$

Reactions of quasi-coherent interaction with  ${}^{28}\text{Si}$  nuclei have been selected via 1.78 MeV characteristic  $\gamma$  radiation following nuclear transition from first excited state  $2_1^+$  into the ground state  $0_{gs}^+$ . The choice of this level was motivated by the results of Monte-Carlo calculations. It was shown that the braking time of Si nucleus after the interaction with a proton is far less than the half-decay period and the shape of the  $\gamma$ -line is not distorted by Doppler effect.

The  $\gamma$  energy essential for the selection of reactions was calculated for all  $1.18 \times 10^6$  registered events via the amplitude  $A_{gd}$  with the help of the calibration dependence (1). The photon energy distribution for the region 1.73÷1.85 MeV is shown in Fig.7.

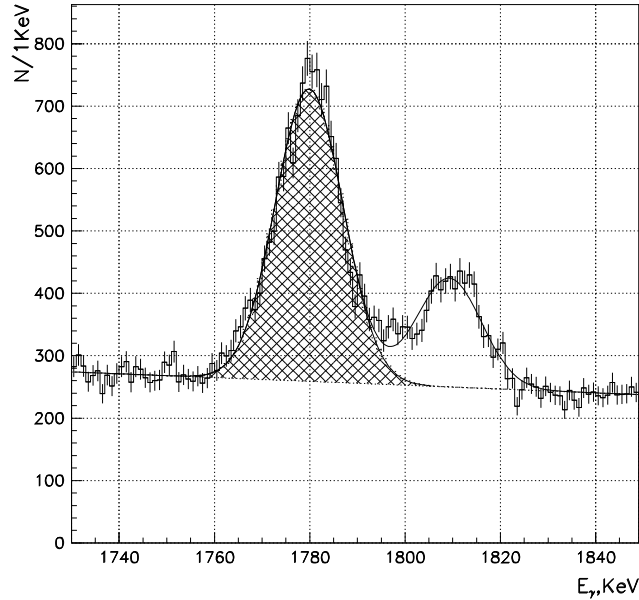


Figure 7:  $\gamma$  energy distribution in  ${}^{28}\text{Si}^*(2_1^+ \rightarrow 0_{gs}^+)$  transition region.

To the right side of the analyzed peak a background signal of reaction  ${}^{28}\text{Si}(p, 2p){}^{26}\text{Mg}^*(2_1^+, 1.809 \text{ MeV})$  with subsequent transition of  ${}^{26}\text{Mg}^*$  nucleus into the ground state can be seen.

The distribution was approximated by a sum of a linear polynomial (background) and two Gaussian functions. The solution found by the method of least squares is shown by smooth lines in Fig.7.

For the analysed peak the mean value of  $\gamma$  energy was found to be  $E_\gamma = (1.7799 \pm 0.0002(\text{stat.}) \pm 0.0010)$  MeV (which is in good agreement with the tabulated value [22]) and the standard deviation -  $\sigma_{E_\gamma} = 7.1$  keV. The number of quasi-coherent events was calculated as the area under the peak (hatched) equal to  $8656 \pm 161$  less background from the reactions  ${}^{29}\text{Si}(p, pn){}^{28}\text{Si}^*$  and  ${}^{30}\text{Si}(p, p2n){}^{28}\text{Si}^*$  equal to  $50 \pm 10$ . It is necessary also to take into

account the probable contribution from the process of  $^{28}\text{Si}$  disintegration by protons in which the de-excitation of the residual nucleus is followed by photon emission in the area  $E_\gamma \pm 2\sigma_{E_\gamma}$ :

$$^{25}\text{Al}(7/2^+, 2.72^{1.775} \rightarrow 3/2^+, 0.944), \quad ^{25}\text{Al}(5/2^+, 1.79^{1.790} \rightarrow 5/2^+, gs), \\ ^{26}\text{Mg}(0^+, 3.589^{1.780} \rightarrow 2^+, 1.809), \quad ^{26}\text{Mg}(4^+, 5.715^{1.775} \rightarrow 3^+, 3.941).$$

Since no experimental data are available on the probabilities of relevant nuclear reactions, in order to estimate the contribution of these reactions the alternative channels of de-excitation with photon emission in the energy range of 50 ÷ 3500 have been used. The upper limit for the contribution was estimated to be 250 events with 67% confidence level for 4 mentioned  $\gamma$ -transitions. Taking into account these corrections we obtain  $N_{1.78} = 8606^{+161}_{-300}$  events.

The cross section of quasi-coherent interaction with the discharge of excited states through 1.78 MeV level has been determined as:

$$\sigma_{1.78} = \frac{4\pi A N_{1.78}}{N_{av} \rho x \Omega_{eff}(E_\gamma) k \xi N_0}, = (37.8^{+0.8}_{-1.5}(stat.) \pm 4.0 (syst.))\text{mb}, \quad (6)$$

where  $A=28$  is the atomic number of the target nucleus;  $N_{av}$  - the Avogadro number,  $\rho=2.20$  g/cm<sup>3</sup> and  $x=2.8$  cm - the density and the thickness of the target;  $\Omega_{eff}(E_\gamma)$  - Ge detector efficiency;  $k=0.65$  -  $\gamma$  absorption coefficient (calculated by the Monte-Carlo method);  $\xi = 1.05$  - the coefficient of *gamma* angle distribution in nuclear transitions  $2^+ \rightarrow 0^+$  [23];  $N_0 = 5.6 \times 10^{10}$  - the number of beam particles reaching the target.

The main peculiarity of first excited level  $^{28}\text{Si}^*(2^+, 1.78)$  is the probable "contribution from above", since at least 10 excited levels with the energy less then the nucleon knock-out energy  $E_t$  have a considerable probability of de-excitation through this level ([22], [24]). Therefore we don't know exactly which excited state resulted from the interaction with protons. However, the comparison of our result with other experimental data allows to make a number of estimations which are presented in the next section.

## 5. The analysis of hadron inclusive quasi-coherent events

### 5.1 . The selection of events

A total of 252163 events with one charged particle (proton mainly) registered in the magnetic spectrometer were selected in all  $\gamma$  energy range.

It was shown by Monte-Carlo calculations that small ( $< 2\%$ ) admixture of  $\pi^+$ -mesons from  $\pi^+\pi^-$  pair production can be present among the registered particles. In order to reject the events without the beam proton interaction with the target, the restriction was imposed on the proton scattering angle with regard to the beam direction:  $\theta > 1.5^0$

For the study of  $^{28}\text{Si}(p, px)^{28}\text{Si}^*$  quasi-coherent reactions events accompanied by 1.78 KeV photon emission which correspond to  $^{28}\text{Si}^*(2_1^+ \rightarrow 0_{gs}^+)$  transition were selected. The photon energy spectrum in the transition area is shown in fig. 8. It is necessary to note once more that all the distributions are efficiency corrected (see section 3.2).

The area  $1760 \leq E_\gamma \leq 1790$  keV chosen for the selection of quasi-coherent events, is marked by dark hatching. To estimate the background contribution, the distribution on the left and right sides from the maximum was approximated by a line. It was obtained

that the number of events in the selected interval is equal to 2380, the background -  $560 \pm 50$ , and the number of quasi-coherent events -  $1820 \pm 50$ . The events on the right and left side from the peak (marked by rare hatching) were used for the establishment of the shape of the background distribution of the nucleus excitation energy and of the other kinematic variables.

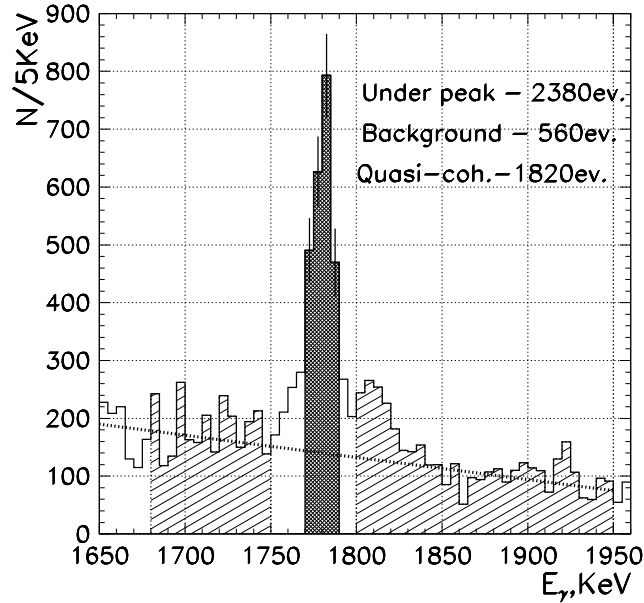


Figure 8:  $\gamma$  energy distribution of one-track events in  $^{28}\text{Si}^*(2_1^+ \rightarrow 0_{gs}^+)$  transition area.

The same calculations have been performed for the events with one charged particle detected in the forward blocks of the proportional chambers PC1 and PC2. Since the angle acceptance was better in this case, a larger number of quasi-coherent events was registered:  $2701 \pm 65$  with the background of  $1435 \pm 45$ .

## 5.2 . Differential cross sections

Differential cross sections have been obtained taking into account three corrections.

1. The efficiency of the selection of one-track events by the MAGOFF code ( $0.61 \pm 0.05$ ). It was estimated via the beam expositions (only one-track events by definition).

2. The missing events with proton scattering at  $\theta > 30^\circ$ . The share of such events was estimated considering the number of events without the response in the proportional chambers. It was found to be 22% from the total number of registered events.

3. The admixture of events with the larger multiplicity of charged particles ( $< 1\%$ ).

Fig.9 shows the differential cross section distribution of 2701 events registered without the momentum measurement (solid line) as well as the distribution of 1820 events with the momentum of  $\geq 0.4$  GeV/c (dotted line). Both distributions are background subtracted.

Their agreement within the statistical errors in the angle range up to  $15^\circ$  points to the absence of noticeable systematic errors in MAGE efficiency.

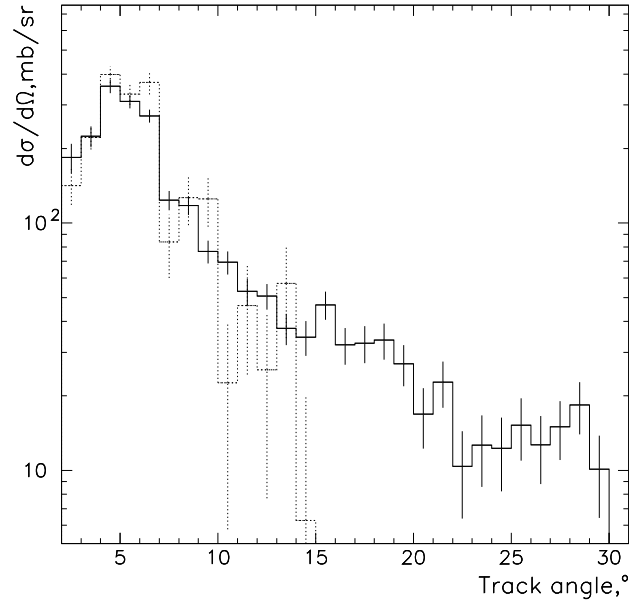


Figure 9: Differential cross section of the reaction  $^{28}\text{Si}(p, px)^{28}\text{Si}^*(E_\gamma = 1.78 \text{ MeV})$  for events detected in the forward chamber blocks PC1 and PC2 (solid histogram) and for events, registered in all blocks of chambers (dotted histogram).

It is interesting to compare the obtained cross sections with the results of other works. The differential cross sections of 1 GeV proton quasi-coherent scattering on  $^{28}\text{Si}$  followed by the excitation of first three levels were measured by LINF group in 1975-1979 at the magnetic spectrometer with the energy resolution of 2 MeV ( see [1], [2]). The integration of this cross section over the proton scattering angles in the interval  $5.7\text{--}15^\circ$  results in the value  $8.9 \pm 0.9 \text{ mb}$  for levels 1.78, 4.61 and 4.96 MeV. Since the transitions from 4.61 and 4.96 levels always proceed through the level 1.78 they are registered in our experiment. Unfortunately, we are not able to separate these reactions because of distortions of  $\gamma$ -spectrum by Doppler effect. However, selecting the events with  $\omega \leq 0.05 \text{ GeV}$  we can estimate in the same angle range the excitation cross section for all  $^{28}\text{Si}$  levels with 1.78  $\gamma$  transition as a final stage of de-excitation process. It was found to be  $\sigma(5.7^\circ \leq \theta \leq 15^\circ, \omega \leq 0.05 \text{ GeV}) = (11.5 \pm 0.5 \pm 1.2) \text{ mb}$  which agree within the limits of two standard deviations with the LINF results. The differential cross-sections of the reaction  $^{28}\text{Si}(p, px)^{28}\text{Si}^*(E_\gamma=1.78 \text{ MeV})$  obtained in our experiment and LINF data are shown in fig.10.

However, the cross-section obtained in our experiment is higher by  $\approx 25\%$  which can be interpreted as an indication of excitation of  $^{28}\text{Si}$  levels with the energy greater than 4.96 MeV in quasi-coherent interactions. The cross section of such processes can be estimated as the difference of two experimental results:

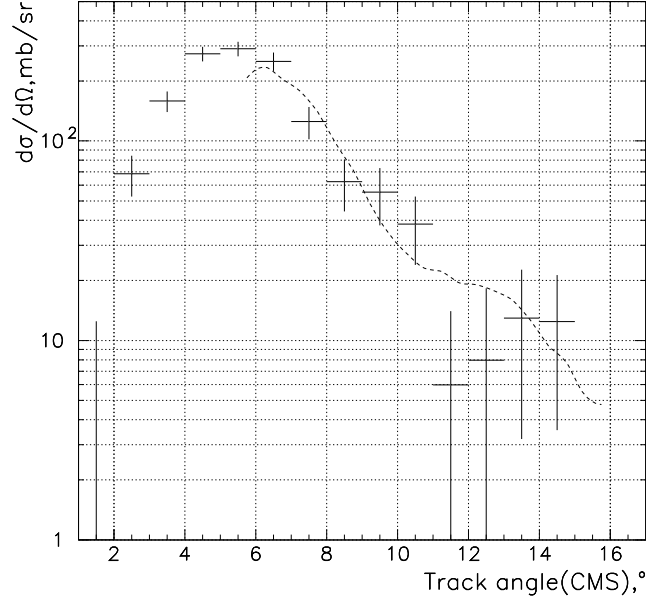


Figure 10: Differential cross section of the  $^{28}\text{Si}(p, px)^{28}\text{Si}^*(E_\gamma=1.78 \text{ MeV})$  reaction in the center of mass system for the events with  $\omega < 0.05 \text{ GeV}$ . LINP result is shown by smooth line.

$$\sigma(5.7^\circ \leq \theta \leq 15^\circ, E^* \geq 4.96) = 2.6 \pm 1.2 \pm 1.2 .$$

### 5.3. Analysis of the excitation energy spectrum. Search for highly excited states

The energy transfer  $\omega$  distribution of 2380 candidates for quasi-coherent events selected in the interval  $1760 \text{ keV} \leq E_\gamma \leq 1790 \text{ keV}$  is shown in fig.11 in logarithmic scale (dotted histogram).

1820 events left after the background subtraction are shown by the hatched histogram. A bulk of events can be seen in the region of small excitation energies  $\omega$ , at larger energies the distribution is more uniform. The arrow in fig.11 indicates the value  $\omega=0.15 \text{ GeV}$  separating two energy regions: the region of non-meson excitation or elastic interactions on the left (1369 events) and the region of possible  $\pi$  - meson production on the right (461 events).

#### 5.3.1. The region of quasi-coherent elastic interactions ( $\omega \leq 0.15 \text{ GeV}$ ).

It was shown above that this region is dominated by the processes of excitation of the first three  $^{28}\text{Si}$  levels with the average energy  $\overline{E_{1-3}^*} = 3.3 \text{ MeV}$ . Since the gap between the levels (3.22 MeV) is far less than the MAGE energy resolution ( $\approx 22 \text{ MeV}$ ), the spectrometer response must have the same shape as the excitation energy resolution function  $g(\overline{E_{1-3}^*}, \omega)$  (5). To take into account the possible contribution from the excitation of higher energy

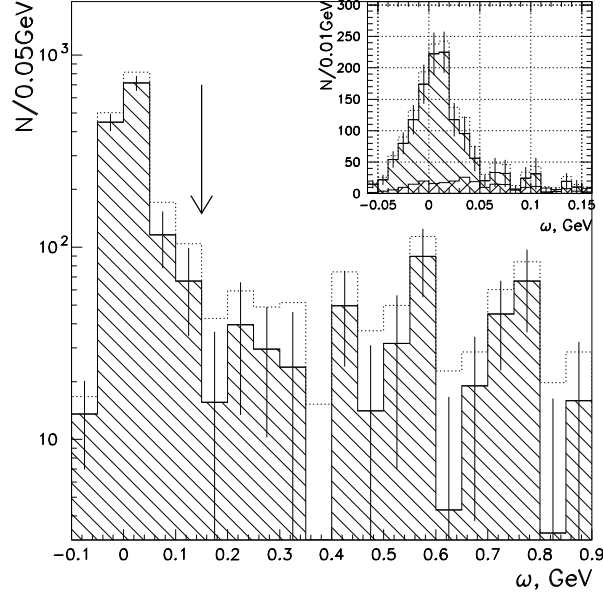


Figure 11:  $\omega$  distribution for  $1760 \text{ keV} \leq E_\gamma \leq 1790 \text{ keV}$ . Hatched is the background subtracted distribution (1820 events). The regions of elastic scattering (left) and unelastic interactions are separated by arrow. In right top corner -  $\omega$  distribution for elastic events with the background (560 events) shown by double hatching.

levels  $\omega$  experimental spectrum has been approximated by the sum of three resolution functions:

$$F = a_1 \cdot g(\overline{E_{1-3}^*}, \omega) + a_2 \cdot g(a_3, \omega) + a_4 \cdot g(a_5, \omega)$$

where the parameters  $a_3$ ,  $a_5$  are responsible for the energies of levels and  $a_1$ ,  $a_2$ ,  $a_4$  - for their possible contributions. The values of parameters were calculated by the maximum likelihood method:  $a_1=147 \pm 46$ ,  $a_2=50 \pm 45$ ,  $a_3=0.013 \pm 0.010$ ,  $a_4=17 \pm 8$ ,  $a_5=0.099 \pm 0.006$ . This solution is presented in fig.12, where the function  $F$  (solid line) and three components marked by figures are superimposed on the experimental histogram.

Except the processes of excitation of first three levels (curve 1), which contribute approximately 70%, the minimization code finds two non-zero contributions in 10 MeV (curve 2) and 100 MeV (curve 3) regions. The contribution from levels with  $4.96 \text{ MeV} \leq E^* \leq E_t$  seems probable enough and don't contradict the conclusion made in section 5.2. In order to test the probability of the existence of nuclear level described by the third component of function  $F$ , the comparative analysis of  $\gamma$  spectra for the events with lower ( $\omega < 0.06 \text{ GeV}$ ) and higher ( $0.06 \text{ GeV} < \omega < 0.15 \text{ GeV}$ ) excitation energies has been made. (see fig. 13).

The selected quasi-coherent events (see section 5.1) displayed in fig.12 as a histogram are marked by hatching. The level of 1.78 MeV is indicated by arrows. The clear maximum is observed for quasi-coherent reactions at small energies (fig.13a). The absence of a noticeable signal in the hatched area in fig.13b indicate that the events observed in the region  $\omega=0.06 \div 0.15 \text{ GeV}$  could be the result of a background fluctuation and can be

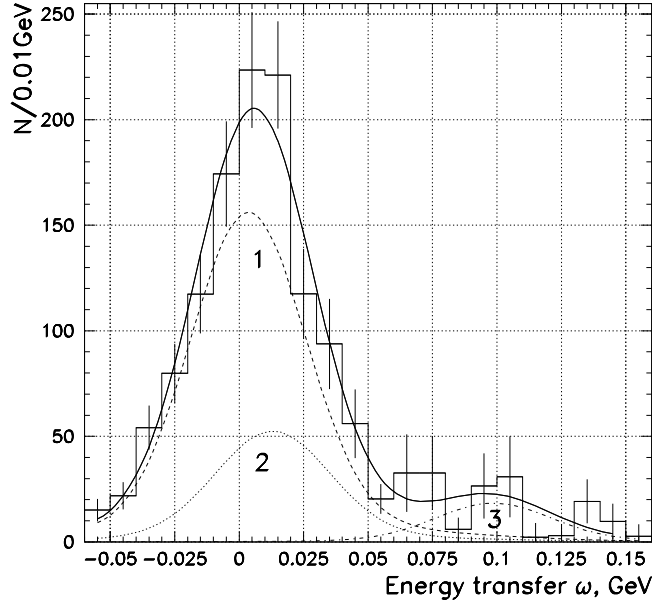


Figure 12: The results of  $\omega$  distribution fit by function  $F$ .

used only to set up the limit on the excitation cross section of long lived nucleus levels. The calculation results are presented in section 5.3.3.

Supposing that the level described by the third component of the function  $F$  is imitated by the background fluctuation, in order to determine the average excitation energy of  $^{28}\text{Si}$  nucleus following quasi-coherent elastic interactions with protons  $\overline{E}^*$  the experimental distribution in the region  $\omega \leq 0.06$  GeV has been described by the resolution function  $F_1 = b \cdot g(\overline{E}^*, \omega)$  only. The estimation of  $\overline{E}^*$  by the least squares method gives  $\overline{E}^* = 0.0053 \pm 0.0014$  GeV with  $\chi^2$  equal to 6.9 for 9 degrees of freedom.

### 5.3.2. The region of $\pi$ -meson production ( $\omega \geq 0.15$ GeV).

In the region  $\omega \geq 0.15$  GeV the proton transfer energy is sufficient for  $\pi$ -meson production. It is known that at proton energies of about 1 GeV  $\pi$ -mesons are produced on free nucleons mainly via the isobars  $P_{33}(1232)(\Delta)$  and  $P_{11}(1440)$  ([25], [26], [27]). Suggesting the same mechanism for  $\pi$ -meson production on quasi-free nucleons in quasi-coherent proton interactions with nuclei, let's estimate the cross-sections. It is shown in [28], [29], [30] that the production of  $P_{11}(1440)$  is strongly suppressed and for the production of  $D_{13}(1520)$  the energy of the incoming proton apparently is not sufficient since the upper limit for the X mass in the reaction  $pp \rightarrow pX$  at  $E=1$  GeV is equal to  $1.43 \text{ GeV}/c^2$ . Therefore the processes of one  $\pi$ -meson production were simulated using  $\Delta$  isobar only and the processes of two  $\pi$ -mesons production - without the participation of isobars.

To estimate the cross section of  $\pi$  - meson production the experimental spectrum has been fitted to a sum of  $\omega$  distributions obtained by Monte-Carlo technique for three



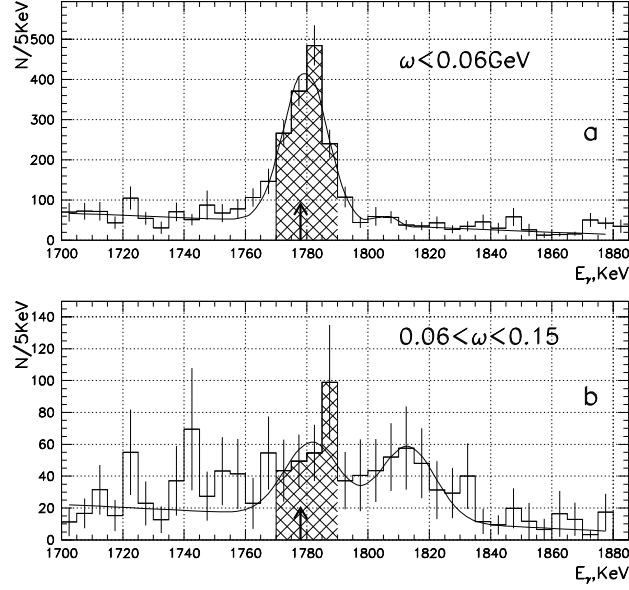


Figure 13:  $\gamma$  energy spectra in the transition region  $^{28}\text{Si}^*(2_1^+ \rightarrow 0_{gs}^+)$  for two excitation energy intervals:  $\omega \leq 0.06$  GeV(a) and  $0.06 < \omega < 0.15$  GeV(b). The energy of the 1.78 MeV transition is indicated by arrows.

processes:

1. Nuclear excitation to the energy  $\overline{E^*}=0.053$  GeV in the reaction  $^{28}\text{Si}(p, p')^{28}\text{Si}^*$ .
2. The isobar production on intranuclear nucleon  $p_f$  ( $n_f$ ) and the decay through well known channels with  $\pi$ -meson production. Seven reactions have been simulated:

$$p + n_f \rightarrow n + \Delta_{1232}^{++} (p\pi^+), \quad [0.47] \quad (1)$$

$$p + p_f \rightarrow p + \Delta_{1232}^+ (p\pi^0), \quad [0.14] \quad (2)$$

$$p + p_f \rightarrow p + \Delta_{1232}^+ (n\pi^+), \quad [0.07] \quad (3)$$

$$p + n_f \rightarrow n + \Delta_{1232}^+ (p\pi^0), \quad [0.11] \quad (4)$$

$$p + n_f \rightarrow n + \Delta_{1232}^+ (n\pi^+), \quad [0.05] \quad (5)$$

$$p + n_f \rightarrow p + \Delta_{1232}^0 (p\pi^-), \quad [0.05] \quad (6)$$

$$p + n_f \rightarrow p + \Delta_{1232}^0 (n\pi^0). \quad [0.11] \quad (7)$$

3. The production of a  $\pi$ -meson pair with the total charge equal to zero on intranuclear nucleon in the following reactions:

$$p + p_f \rightarrow p + p + 2\pi, \quad (8)$$

$$p + n_f \rightarrow p + n + 2\pi. \quad (9)$$

For the simulation of the last 2 processes the Fermi-momentum of the target-nucleon was taken into account. According to the conservation law the total energy of the target-nucleon was accepted to be equal to the rest mass of a free nucleon.

For the reactions (1)-(7) the angle distribution in the center of mass system was simulated according to the results of [26]. The contribution of each reaction obtained from the experimental data on cross section of  $\pi$ -meson production in different isotopic conditions of  $\pi$ N system (see [26], [27], [25]) is given in brackets. The relative contributions of reactions (8) and (9) were accepted to be equal since their simulated  $\omega$  spectra have close shapes. Quasi-coherent events have been selected according to the condition that the nucleon energy after the interaction must be less then the energy of nucleon splitting from  $^{28}\text{Si}$  (0.0116 GeV for proton and 0.0172 for neutron).

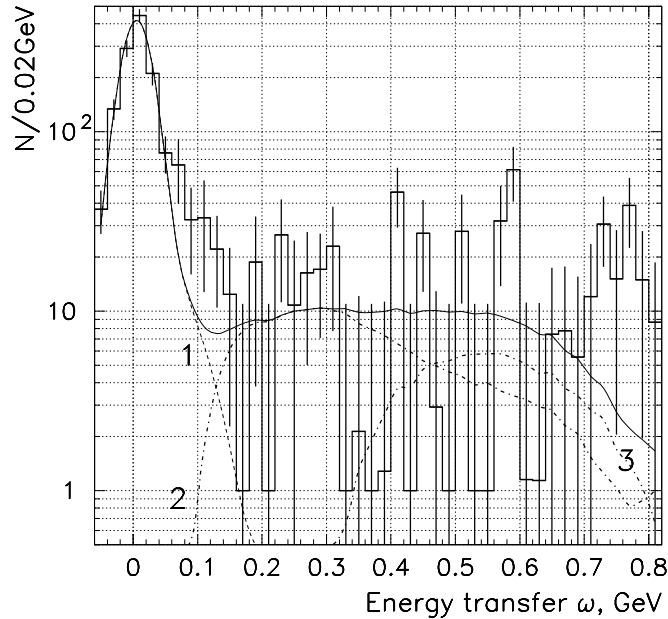


Figure 14:  $\omega$  distribution of quasi-coherent events. Histogram - the experimental data, solid line - the result of data fit by three processes: the nucleus excitation to the energy  $\overline{E^*}=0.053$  GeV (curve 1), the isobar production on intranuclear nucleon (curve 2) and  $\pi$ -meson pair production (curve 3).

The fit was performed without normalization to the total number of events in the experimental histogram. The results are presented in fig.14. The contributions of 3 processes were found to be  $1290 \pm 70$ ,  $198 \pm 70$  and  $92 \pm 60$  respectively. Taking into account the share of events where charged particles are out of the registration region of the spectrometer we obtain the following cross-sections:

$$\begin{aligned}\sigma_1 &= (14.2 \pm 3.0 (stat.) \pm 1.5(syst.)), \\ \sigma_2 &= (7.5 \pm 3.0 (stat.) \pm 0.8(syst.)),\end{aligned}$$

$$\sigma_3 = (3.1 \pm 2.0(stat.) \pm 0.3(syst.)).$$

It should be noted that  $\sigma_1 + \sigma_2 + \sigma_3 = 24.8mb$  provides only the contribution of 2/3 to the total cross section of quasi-coherent scattering (37.8 mb) which indicates the probability of other quasi-coherent processes, in particular, the meson resonance production on a nucleus.

It is interesting to compare the two latest values to the cross sections of the same reactions on free nucleons. As for the quasi-coherent interaction  $\sigma_3/\sigma_2 \approx 40\%$ , for free nucleons this relation is  $< 10\%$ . We can't give valuable explanation to the fact up to now, however the increase in the production of two-pion system following the hadron interactions with nucleus has been observed by a number of recent experiments (see [31], [32]). The mechanism of this phenomenon is not established yet.

### 5.3.3. Limitation on the excitation cross section of high energy levels

It is seen from fig.14 that in several regions of energy transfer the experimental spectrum is not well described with the selected combination of the simulated distributions.

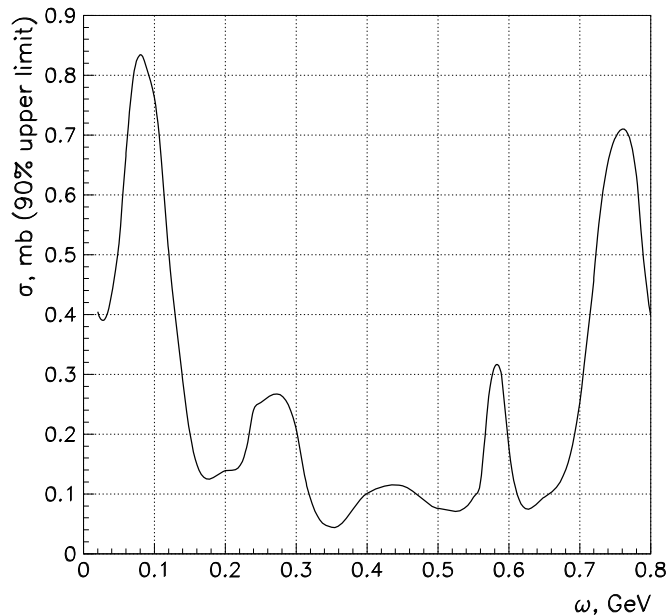


Figure 15: The upper limit of the excitation cross section of high energy levels in quasi-coherent interactions of 1 GeV protons with  $^{28}Si$  at different excitation energies.

One of the regions ( $0.06 \text{ GeV} < \omega < 0.15 \text{ GeV}$ ) in which the excitation of high energy level is probably displayed was mentioned in section 5.3.1. The lack of statistics does not allow to confirm the existence of such levels, it is possible only to impose limits on the probability of the level excitation. The upper limit for this process calculated by the method of least squares at the 90% confidence level is presented in fig.15. It is close to

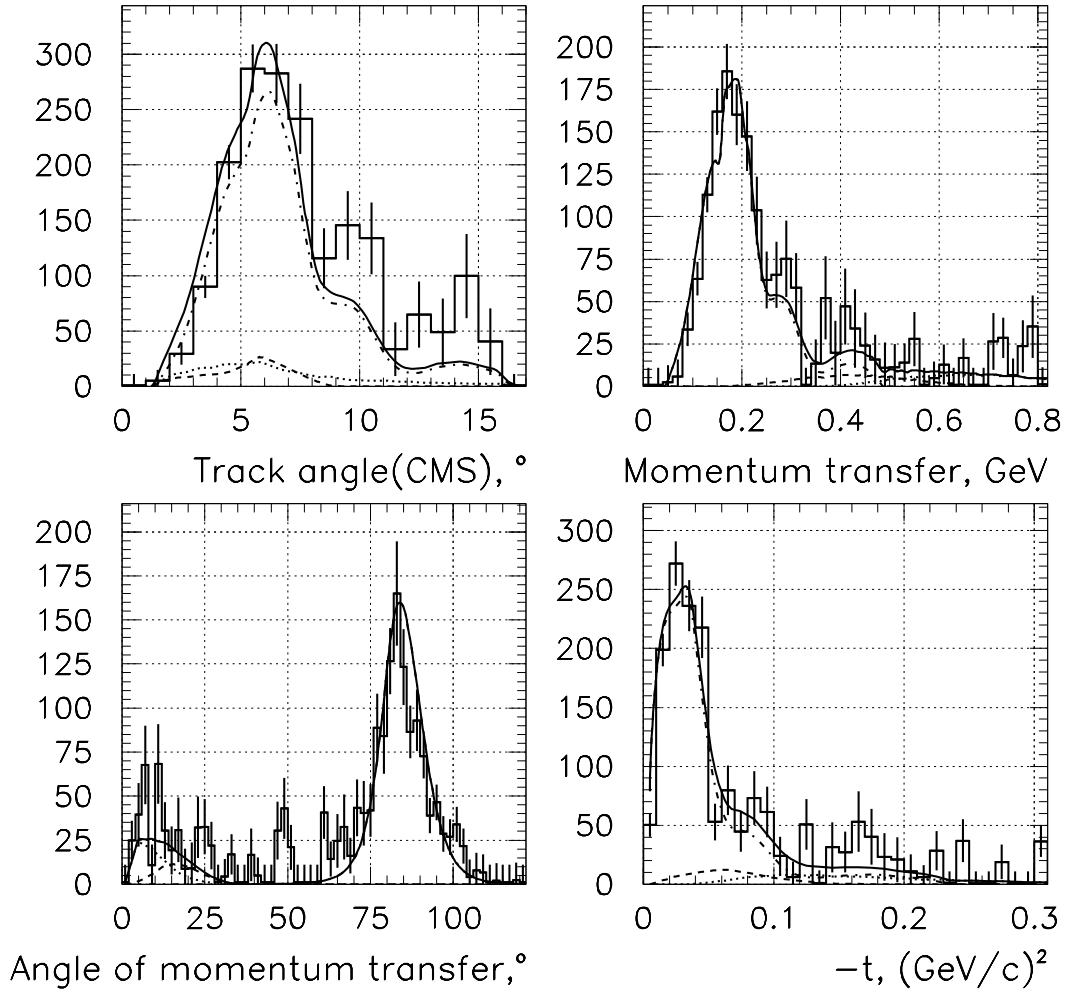


Figure 16: The distributions of a) the proton scattering angle in the center-of-mass system, b) the momentum transfer, c) the angle between the beam direction and the momentum transfer in the laboratory system, and d) the square of transferred 4-th momentum. The simulation results are shown by a smooth line for 3 processes: dash-dot - elastic interaction; dash -  $\Delta$ -isobar production; dot - the production of two  $\pi$ -mesons. The sum of 3 processes is shown by the solid line.

0.1-0.2 mb in the region of 0.3-0.6 GeV and increases to 0.9 mb in the region of 0.1 GeV which points to the excitation of a high level of  $^{28}\text{Si}$  (curve 3 in fig.12). The increase of the upper limit in the region of 0.76 GeV can be possibly explained by  $\pi$ -meson resonance production ( $\rho$  and  $\omega$ ) on the nucleus.

## 5.4 . Other kinematical parameters

The selected quasi-coherent events have been analysed taking into account other kinematical parameters. 4 distributions for 1820 events are presented in fig.16:

a) the proton scattering angle distribution in the  $p\text{-}^{28}\text{Si}$  center of mass system; b) the momentum transfer distribution; c) the distribution of the angle between the beam direction and the momentum transfer in the laboratory system and d) the square of transferred 4-th momentum distribution. The simulation results for 3 processes are shown by smooth lines: dash-dot line - elastic interaction, dash -  $\Delta$ -isobar production, dot - the production of two  $\pi$ -mesons. The sum of 3 processes is presented by solid line. The comparison of the experimental and simulated distributions in fig.14 and fig.16 apparently suggests that the observed quasi-coherent reactions can be described by the sum of three processes in all the region of kinematical variables permitted by kinematical laws.

## 6 . Conclusion

The main results are the following:

1. For the first time the cross sections of quasi-coherent proton interaction with  $^{28}\text{Si}$  have been measured via the registration of  $\gamma$ -transition from the first excited nucleus state to the ground state. The values obtained are:  $37.8_{-1.5}^{+0.8}(\text{stat.}) \pm 4.0$  (syst.)mb for the total cross section,  $14.2 \pm 3.0$  (stat.) $\pm 1.5$ (syst.)mb for elastic cross section and  $23.6 \pm 3.5$  (stat.) $\pm 3.0$ (syst.)mb for non-elastic cross-section.

2. Assuming that single  $\pi$ -mesons are produced on intranuclear nucleons via the isobar  $\Delta(1232)$  and two  $\pi$ -mesons are produced according to the invariant phase volume, the cross sections of these processes have been obtained:  $7.5 \pm 3.0$  (stat.) $\pm 0.8$ (syst.)mb and  $3. \pm 2.$ (stat.)  $\pm 0.3$ (syst.)mb respectively. The two processes summarized give only half contribution to the non-elastic quasi-coherent cross section.

3. The differential cross sections of quasi-coherent interaction have been measured.

4. The upper limit on the cross section of the excitation of long-lived highly excited levels in  $^{28}\text{Si}$  for all the region of energies transferred by proton has been established.

The authors express deep gratitude to the ITEP accelerator operation crew for the presented opportunity of the experiment realization. The authors are thankful to G.A.Leksin, V.B. Gavrilov, A.I. Golutvin, M.G. Schepkin for useful and critical remarks.

## References

- [1] G.D.Alkhazov et al. Experimental data on elastic and inelastic scattering of 1 GeV protons from nuclei. // Leningrad, Preprint LINF, 1979, N531.
- [2] G.D. Alkhazov et al. Scattering of 1 GeV protons on nuclei  $^{28}Si, ^{32}S, ^{34}S$ . // *Yad.Fiz.*, 1975, V.22, I.5, P.902-910.
- [3] G.D.Alkhazov et al. Elastic and inelastic scattering of 1.044 GeV protons by  $^{40}Ca, ^{42}Ca, ^{44}Ca, ^{48}Ca$  and  $^{48}Ti$ . // *Nucl.Phys.*, 1976, V.A274, P.443
- [4] G.D.Alkhazov,A.A.Vorobiev. Investigation of nucleon space distribution in nucleus by method of elastic and inelastic scattering of 1 GeV protons. Diffractive interaction of hadrons with nuclei. Collection of scientific works. / Ahiezer A.I.(editor) et al. Kiev, Nauk.Dumka, 1987, P.5-19.
- [5] G.D.lkhazov et al. Elastic scattering of 1 GeV protons and matter distribution in 1-p shell nuclei. // . *Yad.Fiz.*, 1985, V.42, I. 1(7), P. 9-18.
- [6] Ph.Chomaz,N.Frascaria. Multiple phonon excitation in nuclei: experimental results and theoretical descriptions. // *Phys.Rep.*, 1995, V.252
- [7] A.H.Wuosmaa et al. Evidence for Alpha-Particle Chain Configurations in  $^{24}Mg$ .// *Phys.Rev.Lett.*, 1992, V.68, P.1295–1298.
- [8] E.T.Mirgule et al.  $6\alpha$ -cluster resonance structures in  $^{12}C + ^{12}C$  system and their decay in  $\alpha$  and  $^8Be$  channels.// *Phys.Rev.C*, 1997, V.56, P.1943–1953.
- [9] M.Freer et al.  $^{12}C + ^{12}C$  and  $^{16}O + ^8Be$  decay of  $^{24}Mg$  states excited in the  $^{12}C(^{16}O, ^{24}Mg)\alpha$  reaction. // *Phys.Rev.C*, 1998, V.57, P.1277–1289.
- [10] V.A.Karmanov. High energy hadron scattering on  $^{12}O$  nucleus in framework of nuclear molecular model. // *Yad.Fiz.*, 1982, V.35, I.4, P.848-861.
- [11] W.Bauhoff,H.Schultheis,R.Schultheis. Alpha cluster model and the spectrum of  $^{16}O$ . *Phys.Rev.C*, 1994, V.29, P.1046–1055.
- [12] I.V.Kirpichnikov,V.A.Kuznetsov,A.S.Starostin. Measurement of differential cross section of reaction  $^{16}O(\pi, \pi')^{16}O^*(3^-)$  at the momentum of  $\pi^+$ -meson of 2.0 GeV/c. // M., Preprint ITEP, 1981, N119.
- [13] I.V.Kirpichnikov,V.A.Kuznetsov,A.S.Starostin. Excitation of the nucleus  $^{16}O(6.13$  MeV) by  $\pi^+$ -mesons at the momentum of 2.0 GeV/c. // ., Preprint ITEP, 1984, N94. *Yad.Fiz.*, 1984, V.40, I.6(12), P.1377-1380.
- [14] I.V.Kirpichnikov,V.A.Kuznetsov,A.S.Starostin. Excitation of the nucleus  $^{40}Ca(3.74$  MeV) by 5.0 GeV/c protons. // *Yad.Fiz.*, 1985, V.41, I.1, P.18-20.
- [15] Ascoli G.,Chapin T.J.,Cutler R.et.al. Study of  $\pi^-C \rightarrow (3\pi)^-C(4,44)$  at 6.0 GeV/c. // *Phys.Rev.Lett.*, 1973, 31, N12, P.795–798. Frabetti P.L., Albini E., Bettinazzi T. et. al. Analysis of pion-carbon elastic semicoherent scattering at 40 GeV/c. // Milan, 1979, 7p.(preprint/Milan Institute of Physics: IFUM 231/AE).

- [16] V.L.Korotkih. Quasi-coherent processes of diffractive production of particles with excitation of nucleus levels.// Diffractive interaction of hadrons with nuclei. Collection of scientific works. // Ahiezer A.I.(editor) et al. Kiev, Nauk.Dumka, 1987, P.210-224.
- [17] Yu.D.Bayukov et al.  $A(\pi, \pi\pi)X$  reaction study at 1.4 GeV at small energies transferred to the nucleus and transferred momenta of order of  $p_f$ .// Yad.Fiz., 1992, V. 55, I.12, P. 3261
- [18] A.N. Alekseev et al. Multiwire proportional chambers for wide-resolution spectrometer.// M., Preprint ITEP, 1986, N193. World conference on coordinate detectors in high energy physics. Dubna, 1988, P.217.
- [19] E.T.Bogdanov et al. Electronics for receiving and storing information from big multiwire proportional chambers. // M., Preprint ITEP, 1986, N192.
- [20] P.A. Menshikov et al. System of data read-out from multiwire proportional chambers.// M., Preprint ITEP, 1987, N 178.
- [21] Vasenko A.A. et al.// Questions of atomic science and technique. Materials of 11-th World seminar on precision measurement in nuclear spectroscopy 2-5 Sept 1996, Sarov, P.115.
- [22] R.M.Endt. Energy levels of A=21–44 nuclei (VII). // Nucl.Phys., 1990, V.A521, P.1. (<http://www.nndc.bnl.gov/nndc/nndcnsdd.html>).
- [23] I.V.Kirpichnikov et al. Doppler broadening of gamma-line and the mechanism of excitation of level  $^{12}C(2^+, 4.43MeV)$ . // M., Preprint ITEP, 1984, N96.
- [24] E.V.Lanko,G.S.Dombrowskya, Yu.K.Shkubny. Probabilities of electromagnetic transition of atomic nuclei (Z=1-30). // L., 1972. "Nayka", P. 1-703
- [25] Satoshi Chiba et al. Analysis of proton induced fragment production cross sections by the quantum molecular dynamics plus statistical decay model. // Phys.Rev.C, 1996, V.54, P.285
- [26] Koji Niita et al. Analysis of the  $(N, xN')$  reactions by quantum molecular dynamics plus statistical decay model. // Phys.Rev.C, 1995, V.52, P.2620–2635.
- [27] B.J.VerWest,R.A.Arndt. NN single pion production cross sections below 1500 MeV. // Phys.Rev.C., 1982, V.25, P.1979–1985.
- [28] N.Bianchi et al. Absolute measurement of the total photoabsorption cross section for carbon in the nucleon resonance region. // Phys.Lett., 1993, V.309, P.5–9
- [29] L.A.Kondratyuk et al. Suppression of nucleon resonances in the total photoabsorption on nuclei. // Nucl.Phys., 1994, V.A579, P.453–471.
- [30] N.Bianchi et al. Total hadronic photoabsorption cross section on nuclei in the nucleon resonance region. // Phys.Rev.C, 1996, V.54, P.1688–1699.

- [31] A.Gardestig,G.Falldt,C.Wilkin. Structure in two-pion production in  $dd \rightarrow \alpha X$  reaction. // Phys.Rev.C, 1999, V.59, P.2609–2618.
- [32] F.Bonutti et al. A dependence of the  $(\pi^+, \pi^+\pi^\pm)$  reaction near the  $2 m_\pi$  threshold. // Phys.Rev.Lett., 1996, V.77, P.603– 606.